

Article

Out-of-Plane Sulfur Distortions in the $\text{Bi}_4\text{O}_4\text{S}_3$ Superconductor

Sharon S. Philip¹, Anushika Athauda^{1,†,‡}, Yosuke Goto^{2,†}, Yoshikazu Mizuguchi^{2,†} and Despina Louca^{1,*}

¹ Department of Physics, University of Virginia, Charlottesville, VA 22904, USA; ssp9xc@virginia.edu (S.S.P.); athaudaak@vmi.edu (A.A.)

² Department of Physics, Tokyo Metropolitan University, 1-1 Minami-Osawa, Tokyo 192-0397, Japan; y_goto@tmu.ac.jp (Y.G.); mizugu@tmu.ac.jp (Y.M.)

* Correspondence: louca@virginia.edu

† These authors contributed equally to this work.

‡ Current address: Department of Physics and Astronomy, Virginia Military Institute, Lexington, VA 24450, USA.

Abstract: The local atomic structure of the non-magnetic layered superconductor $\text{Bi}_4\text{O}_4\text{S}_3$ was investigated using neutron diffraction and pair density function (PDF) analysis. Although on average, the crystal structure is well ordered, evidence for local, out-of-plane sulfur distortions is provided, which may act as a conduit for charge transfer from the SO_4 blocks into the superconducting BiS_2 planes. In contrast with $\text{LaO}_{1-x}\text{F}_x\text{BiS}_2$, no sulfur distortions were detected in the planes, which indicates that charge density wave fluctuations are not supported in $\text{Bi}_4\text{O}_4\text{S}_3$.

Keywords: superconductivity; $\text{Bi}_4\text{O}_4\text{S}_3$; local structure distortions; structural analysis; charge transfer; debye temperature



Citation: Philip, S.S.; Athauda, A.; Goto, Y.; Mizuguchi, Y.; Louca, D. Out-of-Plane Sulfur Distortions in the $\text{Bi}_4\text{O}_4\text{S}_3$ Superconductor. *Condens. Matter* **2021**, *6*, 48. <https://doi.org/10.3390/condmat6040048>

Academic Editor: Andrea Perali

Received: 19 October 2021

Accepted: 22 November 2021

Published: 26 November 2021

Publisher's Note: MDPI stays neutral with regard to jurisdictional claims in published maps and institutional affiliations.



Copyright: © 2021 by the authors. Licensee MDPI, Basel, Switzerland. This article is an open access article distributed under the terms and conditions of the Creative Commons Attribution (CC BY) license (<https://creativecommons.org/licenses/by/4.0/>).

1. Introduction

Superconductors with competing ground states have been extensively studied ever since the discovery of the cuprates [1]. Most of the recent interest has been in materials whose parent ground state is magnetic. The bismuth sulfide class of superconductors [2–8], although not magnetic, is a test bed for investigating the effects of charge density wave (CDW) instabilities [9,10], lattice modes leading to phonon softening [9], and spin–orbit (SO) interactions [11,12] on the superconducting mechanism. The BiS_2 superconductors exhibit strong electronic correlations [11]. Density functional theory calculations suggested that spin polarization is present even though the crystal lattice is centrosymmetric [10,11]. Given its quasi-two-dimensional nature, BiS_2 may exhibit SO coupling without breaking crystal inversion symmetry, but instead driven by atomic site asymmetry [11].

Two kinds of superconductors were discovered in the earlier stage, $\text{Bi}_6\text{O}_4\text{S}_4(\text{SO}_4)_{1-x}$ [2] and $\text{LnO}_{1-x}\text{F}_x\text{BiS}_2$ with $\text{Ln} = \text{Pr}, \text{Ce}, \text{La}, \text{and Yb}$ [3,13]. The former consists of a sulfate layer where vacancies and crystal defects are common. The structure is analogous to that of LaOFeAs , an Fe-based superconductor [14]. Superconductivity occurs in the BiS_2 layer that has vacancies, while in the latter, crystal defects induced under pressure have been linked to a higher T_c . The $\text{LnO}_{1-x}\text{F}_x\text{BiS}_2$ system exhibits a peculiar relationship between its structural and superconducting properties where doping with F brings significant disorder to the crystal structure, as well as inducing superconductivity.

In the BiS_2 system, the dominant carriers arise from the Bi 6p orbitals that strongly hybridize with the S 3p orbitals near the Fermi surface. A CDW instability has been proposed in $\text{LnO}_{1-x}\text{F}_x\text{BiS}_2$ that arises from a $(\pi, \pi, 0)$ mode, which corresponds to in-plane displacements of S atoms around the M point [10]. This was verified experimentally in our previous work in [15] on $\text{LaO}_{1-x}\text{F}_x\text{BiS}_2$. The xy-mode of S displacements breaks the long-range symmetry, indicating a long-range CDW state. Whether or not these kinds of distortions exist in the $\text{Bi}_6\text{O}_4\text{S}_4(\text{SO}_4)_{1-x}$ class of materials has not been investigated. The (SO_4) -deficient compound $\text{Bi}_4\text{O}_4\text{S}_3$ corresponding to $x = 0.5$ is superconducting with

$T_c = 4.5$ K [2,16]. Using neutron scattering and pair density function (PDF) analysis, we verified the absence of in-plane S displacements in the BiS_2 superconducting plane of $\text{Bi}_4\text{O}_4\text{S}_3$. This finding points to the absence of the CDW instability, as proposed in $\text{LaO}_{1-x}\text{F}_x\text{BiS}_2$. Instead, an out-of-plane S displacement along the c -axis (0.29 Å in magnitude) is observed, which may lead to a possible charge transfer mechanism from the charge reservoir layers to the superconducting Bi planes. This motion is reminiscent of what was proposed in the cuprate-based superconductor, $\text{YBa}_2\text{Cu}_3\text{O}_{7-\delta}$, in which oxygen motion in the chains above the superconducting CuO_2 layer was attributed to charge transfer [17–19]. The role of out-of-plane S displacement in the charge transfer mechanism for self-doping of the active BiS_2 -layer has been reported in other BiS_2 -based superconductors as well [20,21].

2. Results and Discussion

$\text{Bi}_4\text{O}_4\text{S}_3$ has a tetragonal crystal structure with the $I4/mmm$ space group and lattice parameters $a = b = 3.981$ Å and $c = 41.466$ Å. The refinement results with the neutron powder diffraction data at 2 K fit well using the tetragonal structure. The results are shown in Figure 1a, with a goodness of fit parameter of $R_w = 0.05$. The powder sample contained additional phases of Bi_2S_3 and unreacted bismuth. Shown in Figure 1b is the unit cell of $\text{Bi}_4\text{O}_4\text{S}_3$ with the BiS_2 planes. The three S atom positions along the c axis are labeled S1, S2, and S3, as shown in the diagram for the unit cell. The S2 atoms in the BiS_2 layers lie on the same plane as the Bi atoms, whereas the S1 atom is above the BiS_2 layer, at the apical site. The S3 atoms are part of the SO_4 layer at $z = 0.5$, which is sandwiched by the Bi_2O_2 layers. Defects of SO_4 ions exist in $\text{Bi}_4\text{O}_4\text{S}_3$, the chemical composition being $\text{Bi}_6\text{O}_4\text{S}_4(\text{SO}_4)_{1-x}$ where $x = 0.5$, and the site occupancies of S3 and O atoms in this layer are 0.5 and 0.25, respectively.

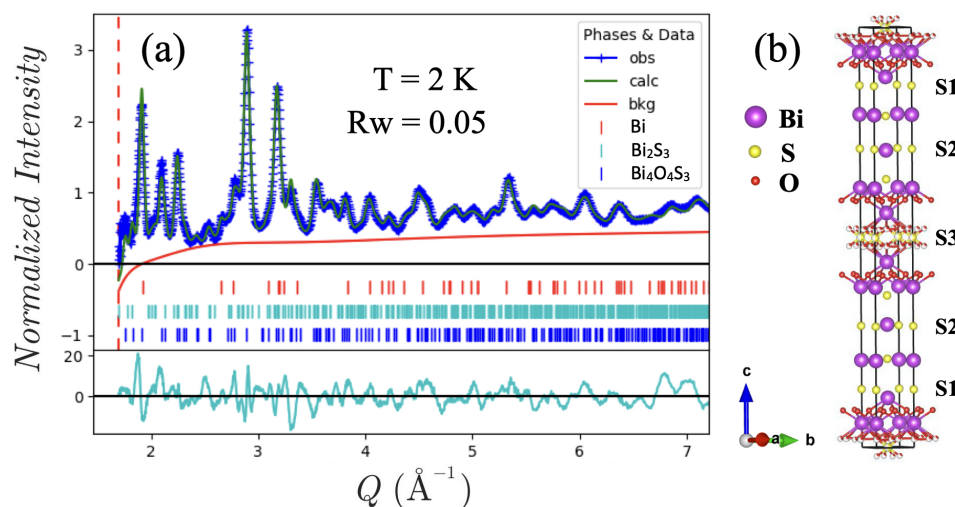


Figure 1. (a) The neutron powder diffraction pattern of $\text{Bi}_4\text{O}_4\text{S}_3$ collected at 2 K. The data are fit well by a tetragonal model with $I4/mmm$ symmetry. Shown on the right in (b) is the model of the crystal structure. The three sulfur atom positions are labeled S1, S2, and S3.

Shown in Figure 2a,b is the temperature dependence of the a and c lattice constants, respectively, obtained from the average structure refinement. Both the a and c lattice constants increase with temperature due to thermal expansion. Figure 2c shows the position z along the c axis within the unit cell for the S1 atom as a function of temperature. The z coordinate is plotted as obtained from both the average and local structure refinement results. The local structure was determined from the PDF by Fourier transforming the powder diffraction spectrum (Bragg peaks + diffuse scattering) into the real space (see the Methods Section). It can be seen that the z coordinate obtained from the local structure refinement is consistently higher than the one obtained from the average crystal structure

refinement, which will be explored further. However, the larger uncertainty in z from PDF refinement suggests that we cannot make inferences on the temperature dependence of the S1 atom displacements from the PDF analysis.

Shown in Figure 2d is the magnetization (M) as a function of temperature in the presence of an applied magnetic field of 10 Oe below 6 K. A large increase in the diamagnetic response of the sample is seen below ~ 4.5 K in the zero-field-cooled (ZFC) magnetization, indicating the onset of superconductivity, in agreement with previous reports [2].

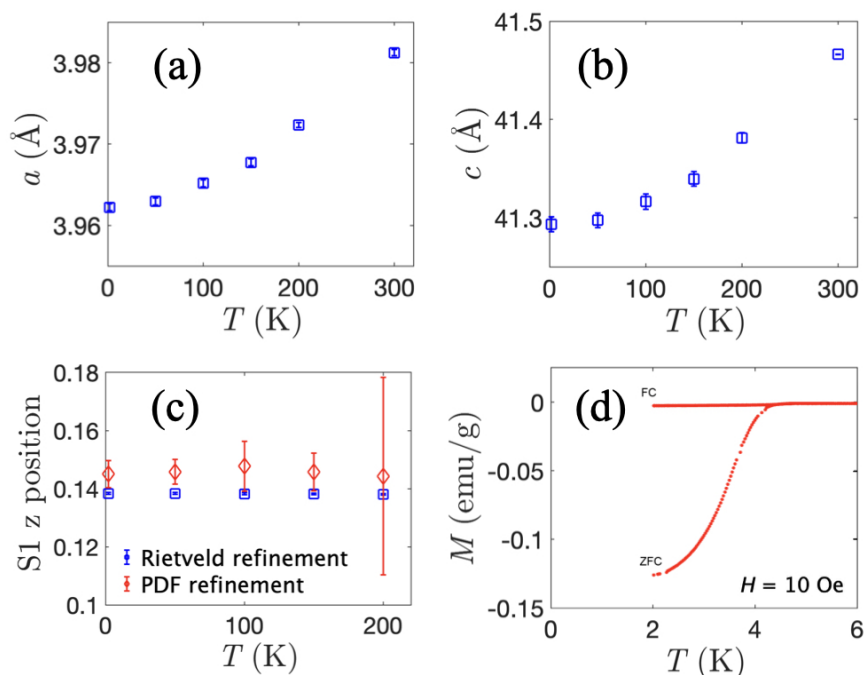


Figure 2. (a) The in-plane lattice constant a and (b) the out-of-plane lattice constant c , both showing the expected positive thermal expansion behavior. (c) A comparison of the z position of sulfur atom S1 obtained from average structure refinement and local structure refinement, plotted as a function of temperature. (d) Low-temperature magnetization for an applied field of 10 Oe. The zero-field-cooling (ZFC) curve shows the superconducting transition below T_c .

Figure 3 shows the results of the PDF analysis, which provides information on the local arrangement of atoms in the real space and is very sensitive to short-range distortions [22,23]. Shown in Figure 3a is a comparison of the reduced pair distribution function $G(r)$ obtained from the experimental data (for $\text{Bi}_4\text{O}_4\text{S}_3$ at 2 K) to $G(r)$ calculated from the “average” model based on the structural parameters obtained from Rietveld refinement. The splitting of the peak at ~ 3 Å, which corresponds to S atom correlations with other atoms, cannot be reproduced using this average model. Figure 3c shows the same experimental data as in Figure 3a, but comparing to a “local” model of $G(r)$ where the S1 and S2 atoms are displaced along the c axis by 0.29 Å and 0.05 Å, respectively. (The calculated peaks below $r = 2$ Å arising from the atom correlations within the sulfate layer are comparable to the noise level of the experimental data.) Figure 3b shows the difference between the average and local models, with arrows marking the displacements of the apical sulfur atom towards the BiS_2 layers in the local model relative to the average model. There is good agreement between the data and the local model. In particular, the splitting of the second peak was reproduced after the apical S atom was displaced from the average-model position. In the local model, the Bi–S bond becomes shorter and the S1 atom moves further from the Bi_2O_2 layer towards the superconducting BiS_2 planes as compared to the average model. This suggests the presence of a charge transfer mechanism, which is reminiscent of what is observed in other layered superconducting systems such as $\text{YBa}_2\text{Cu}_3\text{O}_{7-\delta}$ (YBCO), where the oxygen atom movement towards the CuO_2 planes has been explored [17]. Charge fluctuations are known to exist in materials belonging to the

family of BiS_2 superconductors. $\text{LaO}_{1-x}\text{F}_x\text{BiS}_2$, for instance, shows in-plane short-range distortions of sulfur atoms [15,24]. In $\text{Bi}_4\text{O}_4\text{S}_3$, however, the BiS_2 layer is robust, and no evidence for in-plane distortions or charge fluctuations were found in contrast to other BiS_2 -based superconductors.

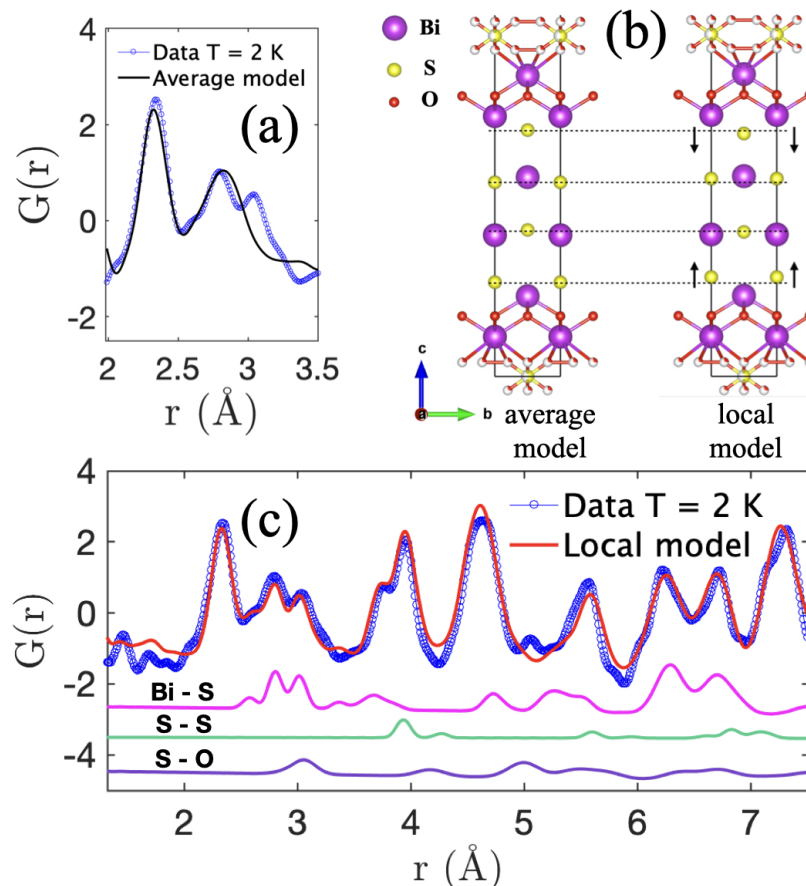


Figure 3. (a) The PDF fit by the average model. (b) The crystal model showing the S1 atom displacement. One half of a unit cell showing the comparison between the average model and local model is shown here. (c) The $G(r)$ function determined for $\text{Bi}_4\text{O}_4\text{S}_3$ at 2 K compared to a local model $G(r)$ indicated by the solid line. The peak splitting at $\sim 3 \text{ \AA}$ is reproduced by the model where the apical S1 atoms move out-of-plane towards the superconducting BiS_2 planes. Partial PDFs representing atom pair correlations between S and either Bi, S, or O atoms are shown.

The effects of the lattice vibrations on the PDF peak widths were modeled using the correlated Debye model [25,26] (see the Methods Section), and the Debye temperature for $\text{Bi}_4\text{O}_4\text{S}_3$ was estimated by studying the mean-squared relative displacements of atomic pair motion as a function of temperature. The PDF peak width FWHM (σ) values from the experimental data were extracted by fitting Gaussian functions to the Bi–O atom pair nearest neighbor correlation peak. Shown in Figure 4 is the temperature dependence of σ^2 fit using the correlated Debye model. The Debye temperature, θ_D , from the model was determined to be 368 K.

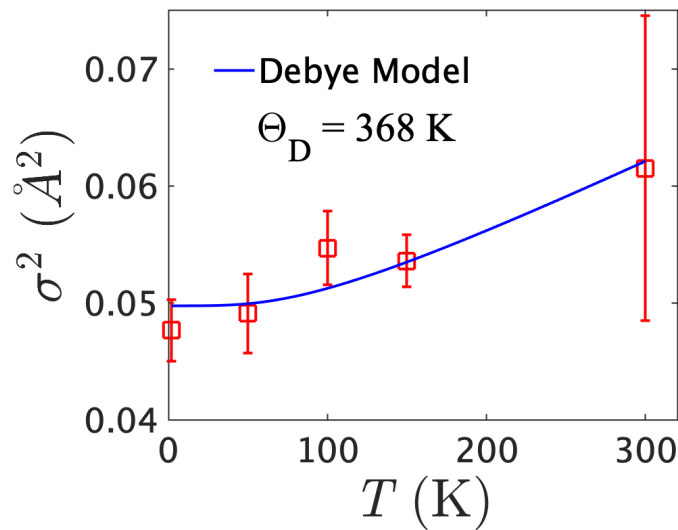


Figure 4. The temperature dependence of squared FWHM values of the PDF peak corresponding to Bi–O correlation in $\text{Bi}_4\text{O}_4\text{S}_3$, extracted from Gaussian fitting. The fit of correlated Debye model is represented by the solid line.

3. Materials and Methods

Polycrystalline samples of $\text{Bi}_4\text{O}_4\text{S}_3$ were prepared by the solid state reaction method using Bi, S, and Bi_2O_3 . The details of the sample preparation were reported in [2]. The temperature dependence of the magnetic susceptibility from 2 K to 6 K was measured in the zero-field-cooled (ZFC) and field-cooled (FC) modes using a superconducting quantum interference device (SQUID) magnetometer with a 10 Oe applied magnetic field.

The time-of-flight (TOF) neutron diffraction experiment was carried out at the Nanoscale Ordered Materials Diffractometer (NOMAD) at the Spallation Neutron Source (SNS) of Oak Ridge National Laboratory (ORNL). The data were analyzed using Rietveld refinement to find parameters characterizing the crystal structure [27], resulting in what we label the “average model”. The PDF analysis [28,29], which provides information on the local arrangement of atoms in the real space without the assumption of periodicity, was performed on the same neutron diffraction data used for the Rietveld refinement. NOMAD is a diffractometer with a large bandwidth of momentum transfer Q , and it provides the total structure function $S(Q)$. $S(Q)$ was Fourier transformed into the real space, as shown in Equation (1), to obtain $G(r)$ [30,31].

$$G(r)_{exp} = \frac{2}{\pi} \int_0^{\infty} Q[S(Q) - 1] \sin(Qr) dQ. \quad (1)$$

The instrument background and empty sample can were subtracted from $S(Q)$, and the data were normalized by vanadium. A maximum Q of 40 \AA^{-1} was used. $G(r)$ corresponds to the probability of finding a particular pair of atoms with an inter-atomic distance r [32].

The crystal structure models were generated using the VESTA software [33]. The correlated Debye model [25,26,34] was used to find the Debye temperature, θ_D , from the temperature dependence of PDF peak widths. Using Equation (2), the full-width at half-maximum (FWHM), defined as σ_{ij} , was extracted from the PDF peak corresponding to the Bi–O nearest neighbor correlations. Here, the Debye wavevector is given by $k_D = (6\pi^2 N/V)^{1/3}$, where N/V is the number density of the crystal; the Debye cutoff fre-

quency is $\omega_D = k_B \theta_D / \hbar$, where k_B is the Boltzmann constant; $\Phi_n = \int_0^{\theta_D/T} x^n (e^x - 1)^{-1} dx$, where x is a dimensionless integration variable.

$$\sigma_{ij}^2 = \frac{6\hbar}{M\omega_D} \left[\frac{1}{4} + \left(\frac{T}{\theta_D} \right)^2 \Phi_1 - \frac{1 - \cos(k_D r_{ij})}{2(k_D r_{ij})^2} - \left(\frac{T}{\theta_D} \right)^2 \int_0^{\theta_D/T} \frac{\sin\left(\frac{k_D r_{ij} T x}{\theta_D}\right) / \left(\frac{k_D r_{ij} T}{\theta_D}\right)}{e^x - 1} dx \right] \quad (2)$$

4. Conclusions

The crystal structure and local atomic distortions in the layered superconductor $\text{Bi}_4\text{O}_4\text{S}_3$ were investigated as a function of temperature. The lattice undergoes a thermal expansion in the temperature range from 2 K to 300 K in both the in-plane and out-of-plane directions. While the average crystal structure is consistent with the $I4/mmm$ space group symmetry across the temperature range, the local structure analysis revealed that the apical S1 atoms move up by 0.29 Å toward the superconducting BiS_2 planes, suggesting a charge transfer mechanism.

Author Contributions: Conceptualization, D.L.; data curation, S.S.P. and A.A.; formal analysis, S.S.P.; funding acquisition, D.L.; investigation, S.S.P.; methodology, S.S.P.; resources, Y.G., Y.M. and D.L.; supervision, D.L.; writing—original draft, S.S.P.; writing—review and editing, D.L. All authors have read and agreed to the published version of the manuscript.

Funding: This research was funded by the U.S. Department of Energy (DOE), Grant Number DE-FG02-01ER45927.

Data Availability Statement: The data presented in this study are available on request from the corresponding author.

Acknowledgments: A portion of this research used resources at the Spallation Neutron Source, a DOE Office of Science User Facility operated by Oak Ridge National Laboratory. We thank John Schneeloch (University of Virginia) for valuable inputs on the manuscript.

Conflicts of Interest: The authors declare no conflict of interest.

References

1. Egami, T.; Louca, D.; McQueeney, R. Nonuniform metallic state in manganites and cuprates. *J. Supercond.* **1997**, *10*, 323–327. [\[CrossRef\]](#)
2. Mizuguchi, Y.; Fujihisa, H.; Gotoh, Y.; Suzuki, K.; Usui, H.; Kuroki, K.; Demura, S.; Takano, Y.; Izawa, H.; Miura, O. BiS_2 -based layered superconductor $\text{Bi}_4\text{O}_4\text{S}_3$. *Phys. Rev. B* **2012**, *86*, 220510. [\[CrossRef\]](#)
3. Mizuguchi, Y.; Demura, S.; Deguchi, K.; Takano, Y.; Fujihisa, H.; Gotoh, Y.; Izawa, H.; Miura, O. Superconductivity in Novel BiS_2 -Based Layered Superconductor $\text{LaO}_{1-x}\text{F}_x\text{BiS}_2$. *J. Phys. Soc. Jpn.* **2012**, *81*, 114725. [\[CrossRef\]](#)
4. Demura, S.; Mizuguchi, Y.; Deguchi, K.; Okazaki, H.; Hara, H.; Watanabe, T.; James Denholme, S.; Fujioka, M.; Ozaki, T.; Fujihisa, H.; et al. New Member of BiS_2 -Based Superconductor $\text{NdO}_{1-x}\text{F}_x\text{BiS}_2$. *J. Phys. Soc. Jpn.* **2013**, *82*, 033708. [\[CrossRef\]](#)
5. Xing, J.; Li, S.; Ding, X.; Yang, H.; Wen, H.H. Superconductivity appears in the vicinity of semiconducting-like behavior in $\text{CeO}_{1-x}\text{F}_x\text{BiS}_2$. *Phys. Rev. B* **2012**, *86*, 214518. [\[CrossRef\]](#)
6. Usui, H.; Suzuki, K.; Kuroki, K. Minimal electronic models for superconducting BiS_2 layers. *Phys. Rev. B* **2012**, *86*, 220501. [\[CrossRef\]](#)
7. Kotegawa, H.; Tomita, Y.; Tou, H.; Izawa, H.; Mizuguchi, Y.; Miura, O.; Demura, S.; Deguchi, K.; Takano, Y. Pressure study of BiS_2 -based superconductors $\text{Bi}_4\text{O}_4\text{S}_3$ and $\text{La}(\text{O},\text{F})\text{BiS}_2$. *J. Phys. Soc. Jpn.* **2012**, *81*, 103702. [\[CrossRef\]](#)
8. Deguchi, K.; Mizuguchi, Y.; Demura, S.; Hara, H.; Watanabe, T.; Denholme, S.; Fujioka, M.; Okazaki, H.; Ozaki, T.; Takeya, H.; et al. Evolution of superconductivity in $\text{LaO}_{1-x}\text{F}_x\text{BiS}_2$ prepared by high-pressure technique. *EPL (Europhys. Lett.)* **2013**, *101*, 17004. [\[CrossRef\]](#)
9. Yildirim, T. Ferroelectric soft phonons, charge density wave instability, and strong electron-phonon coupling in BiS_2 layered superconductors: A first-principles study. *Phys. Rev. B* **2013**, *87*, 020506. [\[CrossRef\]](#)
10. Wan, X.; Ding, H.C.; Savrasov, S.Y.; Duan, C.G. Electron-phonon superconductivity near charge-density-wave instability in $\text{LaO}_{0.5}\text{F}_{0.5}\text{BiS}_2$: Density-functional calculations. *Phys. Rev. B* **2013**, *87*, 115124. [\[CrossRef\]](#)
11. Zhang, X.; Liu, Q.; Luo, J.W.; Freeman, A.J.; Zunger, A. Hidden spin polarization in inversion-symmetric bulk crystals. *Nat. Phys.* **2014**, *10*, 387–393. [\[CrossRef\]](#)

12. Mazziotti, M.V.; Valletta, A.; Raimondi, R.; Bianconi, A. Multigap superconductivity at an unconventional Lifshitz transition in a three-dimensional Rashba heterostructure at the atomic limit. *Phys. Rev. B* **2021**, *103*, 024523. [[CrossRef](#)]
13. Yazici, D.; Huang, K.; White, B.; Chang, A.; Friedman, A.; Maple, M. Superconductivity of F-substituted LnOBiS₂ (Ln = La, Ce, Pr, Nd, Yb) compounds. *Philos. Mag.* **2013**, *93*, 673–680. [[CrossRef](#)]
14. Kamihara, Y.; Watanabe, T.; Hirano, M.; Hosono, H. Iron-based layered superconductor La[O_{1-x}F_x]FeAs (x = 0.05 – 0.12) with T_c = 26 K. *J. Am. Chem. Soc.* **2008**, *130*, 3296–3297. [[CrossRef](#)]
15. Athauda, A.; Yang, J.; Lee, S.; Mizuguchi, Y.; Deguchi, K.; Takano, Y.; Miura, O.; Louca, D. In-plane charge fluctuations in bismuth-sulfide superconductors. *Phys. Rev. B* **2015**, *91*, 144112. [[CrossRef](#)]
16. Singh, S.K.; Kumar, A.; Gahtori, B.; Sharma, G.; Patnaik, S.; Awana, V.P. Bulk superconductivity in bismuth oxysulfide Bi₄O₄S₃. *J. Am. Chem. Soc.* **2012**, *134*, 16504–16507. [[CrossRef](#)]
17. Conradson, S.; Raistrick, I.D. The axial oxygen atom and superconductivity in YBa₂Cu₃O₇. *Science* **1989**, *243*, 1340–1343. [[CrossRef](#)]
18. Bianconi, A.; Saini, N.; Lanzara, A.; Missori, M.; Rossetti, T.; Oyanagi, H.; Yamaguchi, H.; Oka, K.; Ito, T. Determination of the Local Lattice Distortions in the CuO₂ Plane of La_{1.85}Sr_{0.15}CuO₄. *Phys. Rev. Lett.* **1996**, *76*, 3412. [[CrossRef](#)]
19. Bianconi, A.; Lusignoli, M.; Saini, N.; Bordet, P.; Kvik, Å.; Radaelli, P. Stripe structure of the CuO₂ plane in Bi₂Sr₂CaCu₂O_{8+y} by anomalous X-ray diffraction. *Phys. Rev. B* **1996**, *54*, 4310. [[CrossRef](#)]
20. Pugliese, G.; Paris, E.; Capone, F.; Stramaglia, F.; Wakita, T.; Terashima, K.; Yokoya, T.; Mizokawa, T.; Mizuguchi, Y.; Saini, N. The local structure of self-doped BiS₂-based layered systems as a function of temperature. *Phys. Chem. Chem. Phys.* **2020**, *22*, 22217–22225. [[CrossRef](#)]
21. Paris, E.; Mizuguchi, Y.; Wakita, T.; Terashima, K.; Yokoya, T.; Mizokawa, T.; Saini, N. Suppression of structural instability in LaOBiS_{2-x}Se_x by Se substitution. *J. Phys. Condens. Matter* **2018**, *30*, 455703. [[CrossRef](#)]
22. Egami, T.; Petrov, Y.; Louca, D. Lattice effects on charge localization in cuprates. *J. Supercond.* **2000**, *13*, 709–712. [[CrossRef](#)]
23. Louca, D.; Brosha, E.; Egami, T. Structure and lattice defects in LaMnO_{3+δ} and La_{0.96}Sr_{0.04}MnO_{3+δ}. *Phys. Rev. B* **2000**, *61*, 1351. [[CrossRef](#)]
24. Athauda, A.; Yang, J.; Li, B.; Mizuguchi, Y.; Lee, S.; Louca, D. The Crystal Structure of Superconducting LaO_{1-x}F_xBiS₂. *J. Supercond. Nov. Magn.* **2015**, *28*, 1255–1259. [[CrossRef](#)]
25. Beni, G.; Platzman, P. Temperature and polarization dependence of extended x-ray absorption fine-structure spectra. *Phys. Rev. B* **1976**, *14*, 1514. [[CrossRef](#)]
26. Jeong, I.K.; Heffner, R.; Graf, M.; Billinge, S. Lattice dynamics and correlated atomic motion from the atomic pair distribution function. *Phys. Rev. B* **2003**, *67*, 104301. [[CrossRef](#)]
27. Toby, B.H. EXPGUI, a graphical user interface for GSAS. *J. Appl. Crystallogr.* **2001**, *34*, 210–213. [[CrossRef](#)]
28. Proffen, T.; Billinge, S.; Egami, T.; Louca, D. Structural analysis of complex materials using the atomic pair distribution function—A practical guide. *Z. Krist.-Cryst. Mater.* **2003**, *218*, 132–143. [[CrossRef](#)]
29. Proffen, T.; Page, K.L.; McLain, S.E.; Clausen, B.; Darling, T.W.; TenCate, J.A.; Lee, S.Y.; Ustundag, E. Atomic pair distribution function analysis of materials containing crystalline and amorphous phases. *Z. Krist.-Cryst. Mater.* **2005**, *220*, 1002–1008. [[CrossRef](#)]
30. Warren, B.E. *X-ray Diffraction*; Courier Corporation: North Chelmsford, MA, USA, 1990.
31. Peterson, P.; Gutmann, M.; Proffen, T.; Billinge, S. PDFgetN: A user-friendly program to extract the total scattering structure factor and the pair distribution function from neutron powder diffraction data. *J. Appl. Crystallogr.* **2000**, *33*, 1192–1192. [[CrossRef](#)]
32. Egami, T.; Billinge, S.J. *Underneath the Bragg Peaks: Structural Analysis of Complex Materials*; Elsevier: Oxford, UK, 2003.
33. Momma, K.; Izumi, F. VESTA 3 for three-dimensional visualization of crystal, volumetric and morphology data. *J. Appl. Crystallogr.* **2011**, *44*, 1272–1276. [[CrossRef](#)]
34. Philip, S.S.; Yang, J.; Louca, D.; Rosa, P.; Thompson, J.; Page, K. Bismuth kagome sublattice distortions by quenching and flux pinning in superconducting RbBi₂. *Phys. Rev. B* **2021**, *104*, 104503. [[CrossRef](#)]